

Hot nuclear matter with dilatons

G. Kälbermann^a, J. M. Eisenberg^{b,c}, and B. Svetitsky^b

^a*Rothberg School for Overseas Students
and Racah Institute of Physics
Hebrew University, 91904 Jerusalem, Israel*

^b*School of Physics and Astronomy
Raymond and Beverly Sackler Faculty of Exact Sciences
Tel Aviv University, 69978 Tel Aviv, Israel¹*

^c*GSI Darmstadt, Postfach 11 05 52
D-64220 Darmstadt, Germany*

Abstract

We study hot nuclear matter in a model based on nucleon interactions deriving from the exchange of scalar and vector mesons. The main new feature of our work is the treatment of the scale breaking of quantum chromodynamics through the introduction of a dilaton field. Although the dilaton effects are quite small quantitatively, they affect the high-temperature phase transition appreciably. We find that inclusion of the dilaton leads to a metastable high-density state at zero pressure, similar to that found by Glendenning who considered instead the admixture of higher baryon resonances.

¹Permanent address for J.M. Eisenberg

1 Background of the problem

Following upon the early efforts [1, 2] to treat nuclei using relativistic mean-field theory with the exchange of scalar and vector mesons, a great deal of work was done [3–8] to study the consequences of this approach for hot nuclear matter and for neutron stars and supernovae [9, 10]. Within the last few years it has been stressed [11, 12] that since these approaches to the many-nucleon strong-interaction problem must ultimately base themselves on quantum chromodynamics (QCD) they should incorporate such symmetries of QCD as chiral and scale invariance and the breaking of these symmetries there at the quantum level. Both references [11, 12] treat these issues at zero temperature, and it is our purpose here to explore the consequences of incorporating broken scale invariance, or the QCD trace anomaly, at nonzero temperatures. We are interested in particular in temperatures approaching those of the deconfinement phase transition, namely, the range of about 150 to 200 MeV. We employ a scalar field, the dilaton, to represent the effects of glueballs and to mimic the QCD trace anomaly, following a method originally introduced by Schechter [15]. We do not here consider the link between chiral features and the dilaton considered by Mishustin, Bondorf, and Rho [12]: Its main effect is to displace the minimum of the dilaton field from its value when chiral symmetry is respected and the location of that minimum is irrelevant in nuclear matter.

The phase transition found with the present model is obviously not the confinement phase transition, since the degrees of freedom are entirely hadronic. Neither is it the phase transition of chiral symmetry restoration, since our model has no chiral symmetry. There may indeed be three separate phase transitions in the 150–200 MeV temperature range, where the third is the transition studied here: a sharp reduction in the nucleon’s effective mass, accomplished by the self-coupling of the concomitant high density of nucleon-antinucleon pairs. A more extensive model, with the missing degrees of freedom, will show whether two or more of these transitions might coalesce into, say, a single quark–hadron transition.²

Moreover, since the chiral transition is the only one associated with an (almost)

²For a discussion of the relationship between confinement and chiral symmetry phase transitions, see [16].

exact symmetry, it is the only one which assures us that we *must* encounter an actual singularity as we raise the temperature and/or the density. As we shall see, the phase transition studied in this paper occurs (as a function of temperature) only for a limited range of densities. Elsewhere the high- and low-temperature regimes are continuously connected.

Our motivation for studying dilaton effects in hot nuclear matter is to explore the consequences of the fundamental scaling features of QCD within a mean-field model that has had much success in its nuclear applications [17]. The criticism has been voiced [18] that dilaton effects are easily overestimated in nuclear applications if too small a mass is attributed to the glueball in place of values for it in the expected range of 1.5 to 2 GeV. We anticipate that this issue is irrelevant here, because our use of the dilaton in nuclear matter does not require the fixing of a value for the glueball mass. Moreover, quite small changes in energy balance within the regions of phase transition can lead to different qualitative behavior. We find signs of that here.

As this work was being finished, we learned of a parallel calculation being carried out by Papazoglou [19] which reaches similar general conclusions about the role of the dilaton in hot nuclear matter (and also considers extensions to nonzero strangeness). That work considers a particular choice of dynamics for the inclusion of chiral invariance and the nucleon mass is generated by spontaneous symmetry breaking. It is interesting to compare those results with ours since nuclear thermodynamics are very sensitive to any change in the nucleon effective mass.

2 Formalism

Formal features for the handling of hot nuclear matter in mean-field theory have been presented frequently [3–5, 7–12] and we here sketch them only very briefly in order to establish notation and procedures. Our lagrangian is [12, 15]

$$\mathcal{L} = \bar{\psi} \left[i\gamma^\mu (\partial_\mu + ig_\omega \omega_\mu) - \left(\left(\frac{\phi}{\phi_0} \right) M + g_\sigma \sigma \right) \right] \psi + \frac{1}{2} \partial^\mu \sigma \partial_\mu \sigma - V[\sigma, \phi]$$

$$\begin{aligned}
& -\frac{1}{4}(\partial^\mu\omega^\nu - \partial^\nu\omega^\mu)(\partial_\mu\omega_\nu - \partial_\nu\omega_\mu) + \frac{1}{2}m_\omega^2 \left(\frac{\phi}{\phi_0}\right)^2 \omega^\mu\omega_\mu \\
& + \frac{1}{2}\partial^\mu\phi\partial_\mu\phi - U[\phi] ,
\end{aligned} \tag{1}$$

where ψ is the nucleon Dirac field and ω_μ is the field for the vector meson. We use the usual fourth-order polynomial form for the potential of the scalar field σ in the presence of the dilaton ϕ ,

$$V[\sigma, \phi] = \frac{1}{2}m_\sigma^2 \left(\frac{\phi}{\phi_0}\right)^2 \sigma^2 + \frac{1}{3}g_3 \left(\frac{\phi}{\phi_0}\right) \sigma^3 + \frac{1}{4}g_4\sigma^4. \tag{2}$$

The dilaton potential

$$U[\phi] = B \left(e \frac{\phi^4}{\Lambda^4} \log \frac{\phi^4}{\Lambda^4} + 1 \right) \tag{3}$$

yields the usual classical minimum for the field $\phi_0 = \Lambda/e^{1/4}$, where $e \approx 2.718$. The coupling strengths for nucleon-meson couplings are g_σ and g_ω for the scalar and vector fields respectively, and the masses of these fields are m_σ and m_ω . We also require as input parameters here the coefficients g_3 and g_4 in the scalar potential. The powers of ϕ appearing in eqs. (1) and (2) are determined, as usual, by the dimensionality of the term in question.

The mean-field equations in infinite nuclear matter are given by

$$g_\sigma\rho_s + m_\sigma^2 \left(\frac{\phi}{\phi_0}\right)^2 \sigma + g_3 \left(\frac{\phi}{\phi_0}\right) \sigma^2 + g_4\sigma^3 = 0 \tag{4}$$

for the scalar field,

$$g_\omega\rho_v - m_\omega^2 \left(\frac{\phi}{\phi_0}\right)^2 \omega = 0 \tag{5}$$

for the vector field with only the time component ω present, and

$$M\rho_s + \frac{1}{3}g_3\sigma^3 + 4B \left(\frac{\phi}{\phi_0}\right)^3 \left(1 + \log \frac{\phi^4}{\Lambda^4}\right) = m_\omega^2 \left(\frac{\phi}{\phi_0}\right) \omega^2 - m_\sigma^2 \left(\frac{\phi}{\phi_0}\right) \sigma^2 \tag{6}$$

for the nucleon. Here the nuclear scalar and vector densities for nonzero temperatures are

$$\rho_s = 4 \int \frac{d^3p}{(2\pi)^3} \frac{M^*}{\sqrt{p^2 + M^{*2}}} (n_p^+ + n_p^-) \tag{7}$$

and

$$\rho_v = 4 \int \frac{d^3p}{(2\pi)^3} (n_p^+ - n_p^-) . \tag{8}$$

The factor 4 appearing in eqs. (7) and (8) is for nucleon degeneracy. The fermion and antifermion distributions are

$$n_p^\pm = \frac{1}{1 + \exp [(\epsilon_\pm(p) \mp \mu) / T]} . \quad (9)$$

Here the nucleon and antinucleon energies are given by

$$\epsilon_\pm = \sqrt{p^2 + M^{*2}} \pm g_\omega \omega \quad (10)$$

and the nucleon effective mass is

$$M^* = \left(\frac{\phi}{\phi_0} \right) M + g_\sigma \sigma. \quad (11)$$

These equations are now solved for given values of the temperature. Once this is accomplished, the system energy density is

$$\begin{aligned} \mathcal{E} = & 4 \int \frac{d^3p}{(2\pi)^3} \sqrt{p^2 + M^{*2}} (n_p^+ + n_p^-) + V[\sigma, \phi] + U[\phi] \\ & + \frac{1}{2} \left(m_\omega \left(\frac{\phi}{\phi_0} \right) \right)^{-2} g_\omega^2 \rho_v^2 , \end{aligned} \quad (12)$$

and the pressure is

$$\begin{aligned} P = & \frac{1}{3} \cdot 4 \int \frac{d^3p}{(2\pi)^3} \frac{p^2}{\sqrt{p^2 + M^{*2}}} (n_p^+ + n_p^-) - V[\sigma, \phi] - U[\phi] \\ & + \frac{1}{2} \left(m_\omega \left(\frac{\phi}{\phi_0} \right) \right)^{-2} g_\omega^2 \rho_v^2 . \end{aligned} \quad (13)$$

Thermodynamic properties of hot nuclear matter are most easily discussed in terms of the three intensive variables that characterize the mixed phases near a transition, namely, the pressure P , temperature T , and chemical potential μ . This immediately recommends the use of the grand potential [20, 21]

$$\omega(\mu, T) = \frac{1}{V} \Omega(\mu, T) = -P . \quad (14)$$

Near a phase transition we then have thermodynamic equilibrium for that branch having highest pressure (minimal grand potential) at given chemical potential and temperature. Thus we show our results as functions of chemical potential rather than baryon density so that transition points may easily be read off the pressure curves and applied to the other thermodynamic variables.

At the temperatures of interest, a pion gas coexists with the nucleon gas we are studying. Its mean field is zero, and it affects the nucleon gas through scattering. Its treatment is beyond the scope of our mean-field approach.

3 Results and discussion

We fix parameters, basing ourselves on previous work [9], such that at nuclear saturation the density is $\rho_0 = 0.153 \text{ fm}^{-3}$, the binding energy per nucleon is $E_B = -16.5 \text{ MeV}$, and the compressibility is $K = 212 \text{ MeV}$ when the dilaton is not present and $K = 234 \text{ MeV}$ when it is. The nucleon’s effective mass is $M^* = 0.57 M$. The parameters of eqs. (1) and (2) are then $g_\sigma = 10.1$, $g_\omega = 13.3$, $m_\sigma = 492 \text{ MeV}$, and $m_\omega = 795 \text{ MeV}$ for the scalar and vector mesons, and $g_3 = -12.2 \text{ fm}^{-1}$ and $g_4 = -36.3$ for the scalar potential, for the case where the dilaton is absent. When it is present the scalar meson coupling becomes $g_\sigma = 9.6$ and the “bag” constant for the dilaton field is taken to be $B = (200 \text{ MeV})^4$, as in [11].³ For nuclear matter the value of the dilaton mean field ϕ_0 , or alternatively of the glueball mass, is not required since we express all quantities in the equations of motion in terms of the ratio ϕ/ϕ_0 . We note that the scalar potential V of eq. (2) used here suffers from the problem of “bifurcation,” which is well known in this area [4, 8]: In order to obtain reasonable values for the nuclear compressibility K we are obliged to use negative, and therefore destabilizing, coefficients g_3 and g_4 . One must keep in mind that our Lagrangian is after all that of an effective field theory.

Figure 1 shows the well-known [6, 22] gas–liquid phase transition that occurs in these mean-field models at low temperatures. Not surprisingly, there is hardly a discernible difference between the cases with and without dilaton for these low values of T .

We now consider the higher-temperature regime where there appear larger quantitative differences between the two cases. In the theory *with* dilatons, there is a

³The relative ease with which successful parameters are found in this model comes about because we have not constrained it to fit properties of finite nuclei [13, 14]. We are satisfied with studying dilaton effects on a model which describes well zero-temperature nuclear matter, and thus we have not explored the parameter space more fully.

first-order phase boundary in the T - μ plane extending from the T axis at $T \simeq 185$ MeV to a critical point at $(T, \mu) \simeq (170 \text{ MeV}, 565 \text{ MeV})$. In the theory *without* dilatons, the intercept is at⁴ $T \simeq 189$ MeV, with a critical endpoint at $(T, \mu) \simeq (185 \text{ MeV}, 300 \text{ MeV})$. Figures 2 and 3 show isotherms of pressure and energy density as functions of chemical potential. The phase transition is clearly visible as a crossing of pressure curves and as a discontinuity in the energy density. To characterize the phases we display the effective nucleon mass in Fig. 4. The low (T, μ) regime is a *normal* phase, by which we mean a state with an effective nucleon mass close to that of zero-temperature, ordinary nuclear matter. The phase at large T or large μ is an *abnormal* phase in that the nucleon's effective mass is much smaller. For $T = 100$ and 150 MeV, one sees a smooth crossover between the two regimes as μ is varied; a phase transition appears in the isotherms when one crosses the phase boundary just described. For sufficiently large T the system is abnormal for all μ .

Since there are small changes in the parameters between the models with and without dilatons one should not take the differences in temperature very seriously. On the other hand, the abnormal states above the transition region show a rather smaller effective mass (Fig. 4) in the presence of the dilaton than they exhibit in its absence. This is because when the dilaton is involved it provides an additional mechanism to that of the scalar field for reducing the nucleon mass above the transition region, as may be seen in eq. (11). The low effective mass that is found at and above the transition region is the characteristic feature of the abnormal branch. The occurrence of this abnormal feature is a consequence here [6] of a feedback loop whereby at high temperatures many nucleon-antinucleon pairs may be produced, which in turn enhances the scalar field [see eqs. (4) and (7)], thus further lowering the effective mass. In the presence of the dilaton, the ϕ field also participates in this loop through eq. (6). As is well known [23], there is an alternative mechanism which produces an abnormal state at *low* temperatures purely through the increase in baryon density.

The most important consequence of the dilaton is in the metastable extension of the abnormal phase to low values of μ . As seen in Fig. 2, both with and without the

⁴Due to numerical difficulties we have not really verified that the phase boundary intersects the T axis in the theory without dilatons.

dilaton the metastable state persists all the way down to $\mu = 0$ (whence it continues into the $\mu < 0$ region since $\mu \rightarrow -\mu$ is a symmetry of the theory). In the model *with* the dilaton, however, the metastable state crosses $P = 0$ which implies that a nugget of this phase is mechanically stable. This feature was discovered by Glendenning [6] in a model *without* dilatons which included the contributions of a ladder of baryonic resonances to the thermodynamics. We can only speculate that inclusion of *both* the dilaton and the baryonic resonances will serve to drive the zero-pressure state towards higher μ and hence closer to the phase transition, thus improving prospects for observability. We note, however, that the metastable states in Fig. 2, for both models, are separated from the true minimum of the grand potential at the same μ (the stable phase) by a very low barrier. This does not make us sanguine regarding the lifetime of the state.

We also present curves for the baryon density (Fig. 5) and the dilaton field expectation value (Fig. 6). The latter shows a slow decrease as μ increases and then a jump to the abnormal state in which the dilaton field drops by some 10%.

In sum it appears that the incorporation of scale-invariance breaking in a form suggested by QCD can have significant effects in the phase structure of hot nuclear matter. We hope that this observation may be of particular use in the study of effects of a hot hadronic medium on baryon behavior. This has been explored, for example, using skyrmions [24], though thus far without consideration of dilaton effects. Since such effects have been found to be important for one- and two-skyrmion systems [25] it will be important to take the dilaton into account in both its roles in eventual studies of baryons immersed in hot matter.

It is a pleasure to acknowledge very useful conversations on the subject matter of this paper with Walter Greiner, Igor Mishustin, Panajotis Papazoglou, and Horst Stöcker. Part of this work was carried out while JME was visiting the Institut der Theoretische Physik der Universität Frankfurt, and he wishes to express his gratitude for the very kind hospitality he received there. BS thanks the Weizmann Institute of Science for its continuing hospitality. This work was funded in part by the Israel Science Foundation, by the U.S.-Israel Binational Science Foundation, and

by the Ne'eman Chair in Theoretical Nuclear Physics at Tel Aviv University.

References

- [1] L.D. Miller and A.E.S. Green, *Phys. Rev. C* 5 (1972) 241.
- [2] J.D. Walecka, *Ann. Phys.* 83 (1974) 491.
- [3] J. Boguta, *Phys. Lett. B* 109 (1982) 251.
- [4] J. Boguta and H. Stöcker, *Phys. Lett. B* 120 (1983) 289.
- [5] J. Theis, G. Graebner, G. Buchwald, J.A. Maruhn, W. Greiner, H. Stöcker, and J. Polonyi, *Phys. Rev. D* 28 (1983) 2286.
- [6] N.K. Glendenning, *Nucl. Phys. A*469 (1987) 600.
- [7] B.M. Waldhauser, J. Theis, J.A. Maruhn, H. Stöcker, and W. Greiner, *Phys. Rev. C* 36 (1987) 1019.
- [8] B.M. Waldhauser, J.A. Maruhn, H. Stöcker, and W. Greiner, *Phys. Rev. C* 38 (1988) 1003.
- [9] K. Sumiyoshi and H. Toki, *Ap. J.* 422 (1994) 700.
- [10] K. Sumiyoshi, H. Kuwabara, and H. Toki, *Nucl. Phys. A*581 (1995) 725.
- [11] R.G. Rodriguez and J.I. Kapusta, *Phys. Rev. C* 44 (1991) 870.
- [12] I. Mishustin, J. Bondorf, and M. Rho, *Nucl. Phys. A*555 (1993) 215.
- [13] R. J. Furnstahl and B. D. Serot, *Phys. Lett. B* 316 (1993) 12.
- [14] E. K. Heide, S. Rudaz, and P. J. Ellis, *Nucl. Phys. A*571 (1994) 713.
- [15] J. Schechter, *Phys. Rev. D* 21 (1980) 3393.
- [16] B. Svetitsky, *Phys. Rep.* 132 (1986) 1.
- [17] B.D. Serot and J.D. Walecka, *Adv. Nucl. Phys.* 16 (1986) 1, ed. J. Negele and E. Vogt (Plenum, New York, 1986).

- [18] M.C. Birse, J. Phys. G 20 (1994) 1287.
- [19] I. Mishustin, P. Papazoglou, and H. Stöcker, private communication; P. Papazoglou, diploma thesis, Institute for Theoretical Physics, University of Frankfurt, July, 1995.
- [20] D. ter Haar and H. Wergeland, *Elements of thermodynamics* (Addison–Wesley, Reading, Massachusetts, 1966) pp. 68-69.
- [21] R. Kubo, *Thermodynamics* (North-Holland, Amsterdam, 1968) p. 136.
- [22] J.D. Walecka, Phys. Lett. B 59 (1975) 109.
- [23] T.D. Lee and G.C. Wick, Phys. Rev. D 9 (1974) 2291.
- [24] I. Mishustin, Sov. Phys. JETP 71 (1990) 21.
- [25] J.M. Eisenberg and G. Kälbermann, in *Progress in Particle and Nuclear Physics, volume 36*, ed. A. Faessler (Elsevier–Oxford), to be published.

Figure captions

Figure 1. Pressure P versus chemical potential μ at low temperatures $T = 8$ MeV (right) and 10 MeV (left) in the region of the gas–liquid phase transition: (a) no dilaton, (b) with dilaton. Dashed segments represent metastable states.

Figure 2. Pressure P versus chemical potential μ at the high-temperature phase transition: (a) without dilaton, at $T = 188$ MeV; (b) with dilaton, at $T = 175$ MeV.

Figure 3. Energy density \mathcal{E} versus chemical potential μ for values of temperature spanning the phase transition region: (a) No dilaton. The isotherms represent, from bottom to top, $T = 100, 150, 186, 188,$ and 190 MeV. (b) With dilaton. Temperatures, from bottom to top, are $T = 100, 150, 172, 175,$ and 200 MeV.

Figure 4. Nucleon effective mass M^* versus chemical potential μ for values of temperature spanning the phase transition region: (a) no dilaton, (b) with dilaton. The temperature values are the same as in Fig. 3, but in the opposite order: top to bottom.

Figure 5. Baryon density ρ_v versus μ : (a) no dilaton, $T = 188$ MeV; (b) with dilaton, $T = 175$ MeV.

Figure 6. Dilaton field ϕ/ϕ_0 for $T = 175$ MeV.

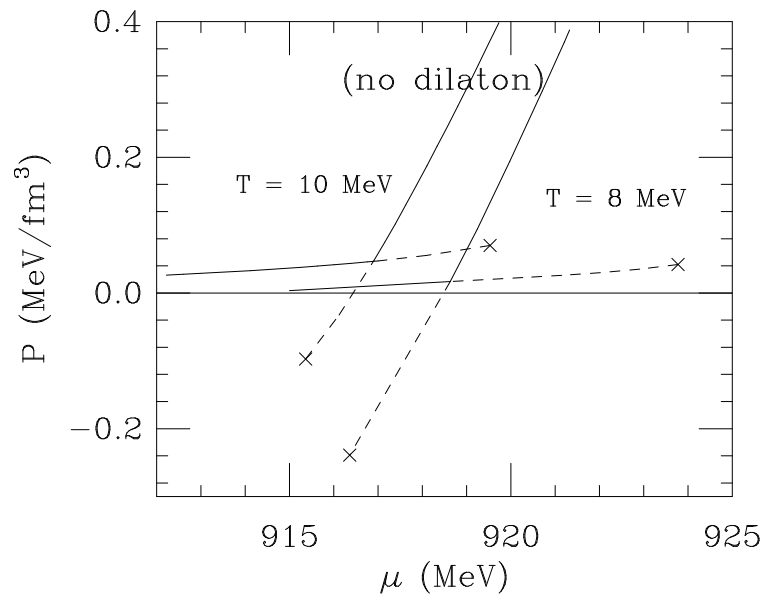


Fig. 1(a)

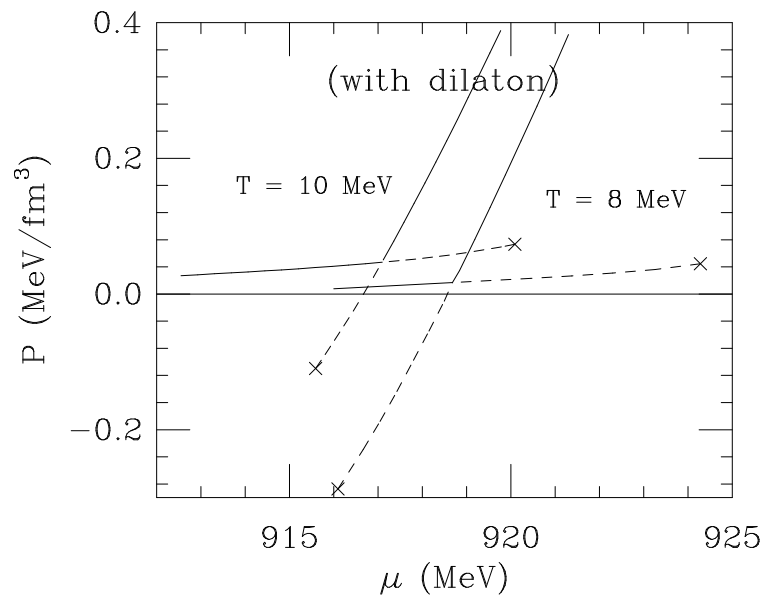


Fig. 1(b)

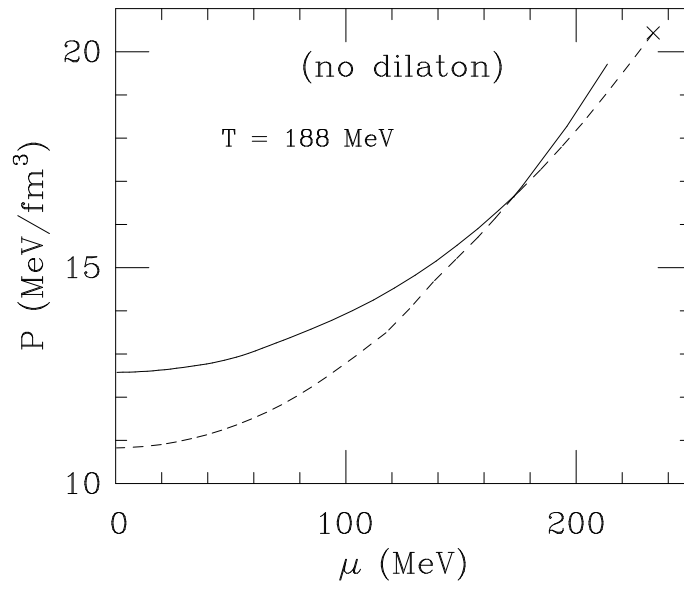


Fig. 2(a)

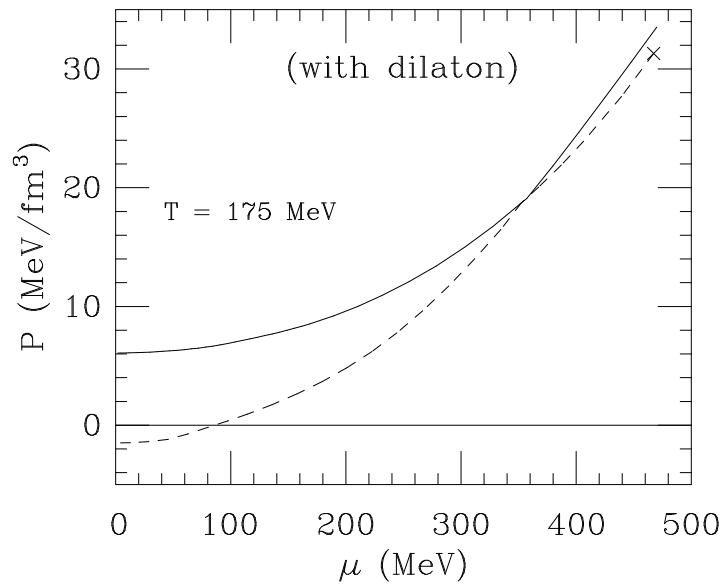


Fig. 2(b)

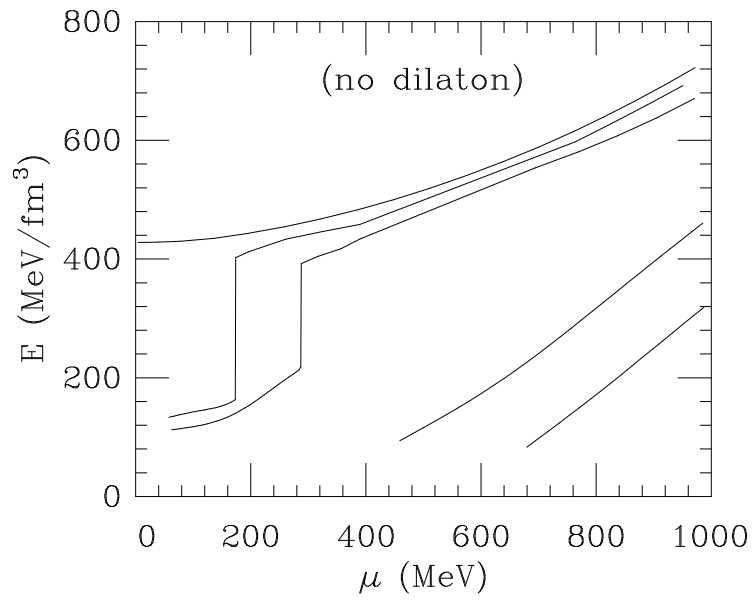


Fig. 3(a)

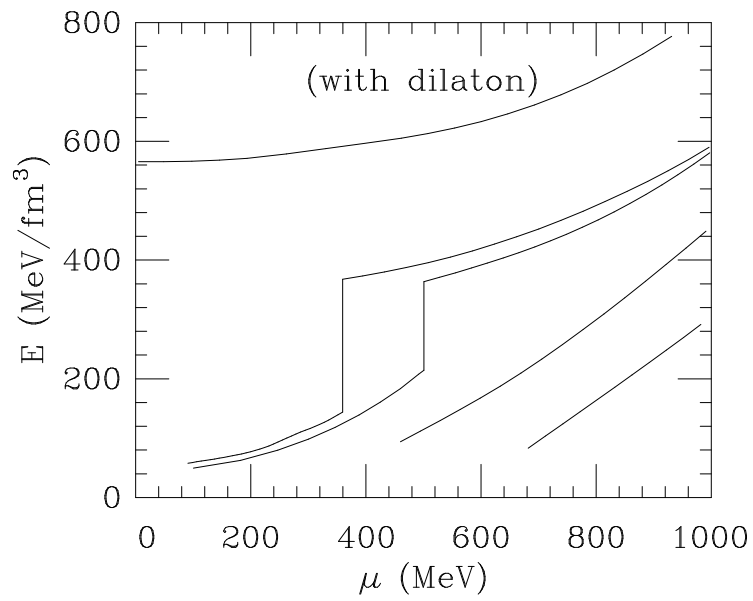


Fig. 3(b)

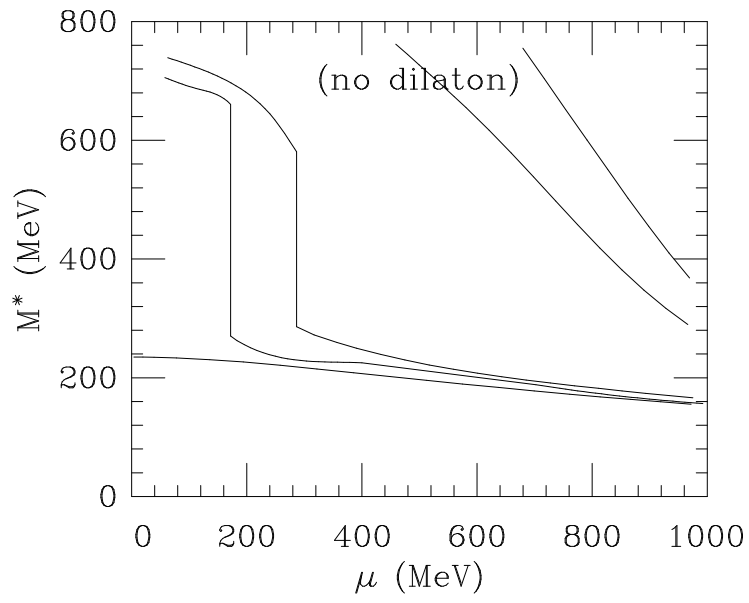


Fig. 4(a)

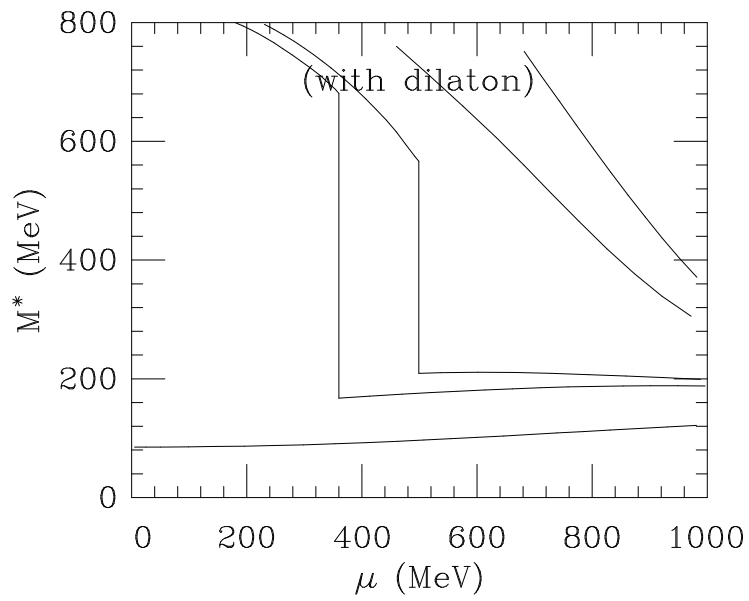


Fig. 4(b)

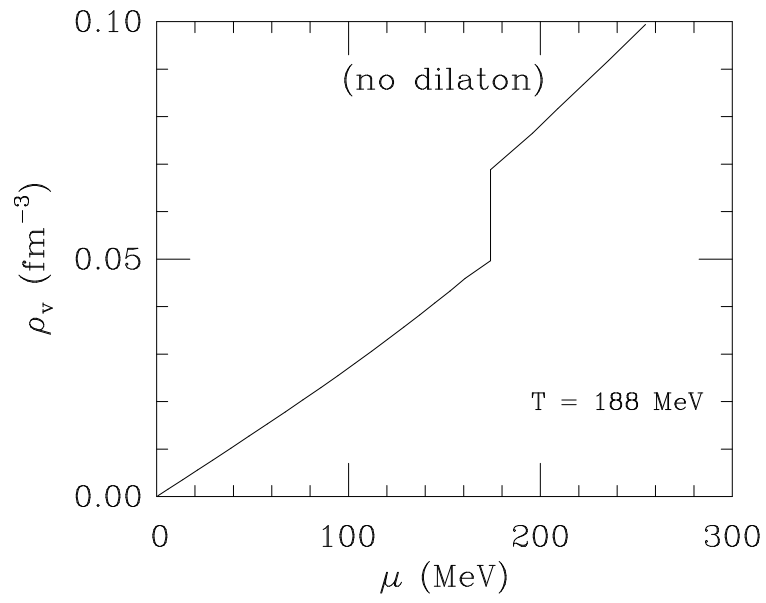


Fig. 5(a)

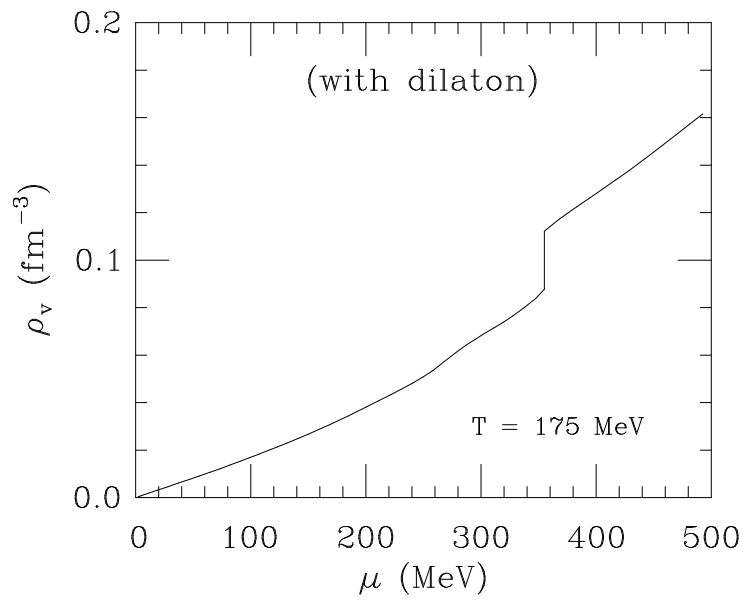


Fig. 5(b)

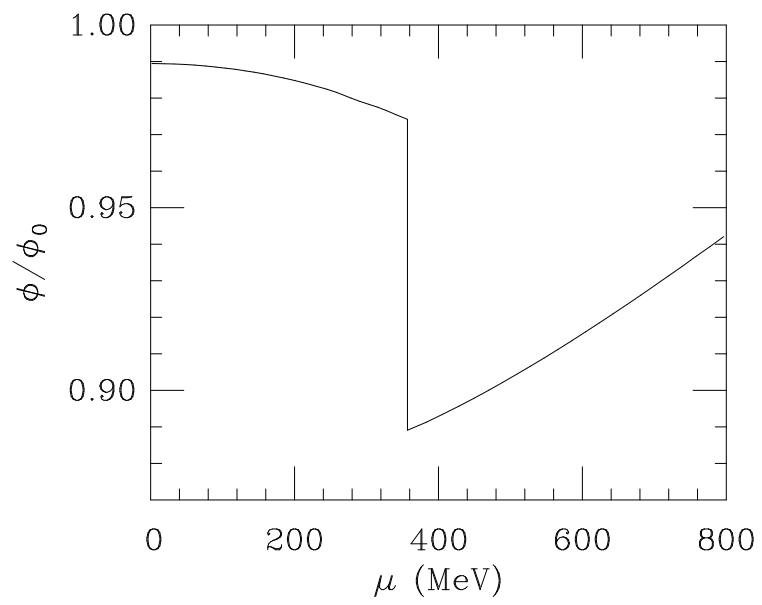


Fig. 6